RSC Advances

ROYAL SOCIETY OF CHEMISTRY

www.rsc.org/advances

Journal Name

RSCPublishing

ARTICLE

Role of HA Additive in Quantum Dot Solar Cell with $Co[(bpy)_3]^{2+/3+}$ Based Electrolyte

Cite this: DOI: 10.1039/x0xx00000x

Sang Youn Chae,[a,b] Yun Jeong Hwang,[a,c**] Oh-Shim Joo[a*]

Received 00th January 2012,
Accepted 00th January 2012

DOI: 10.1039/x0xx00000x

www.rsc.org/

A strategy to improve the power conversion efficiency (η) in a quantum dot solar cell (QDSC) is demonstrated with a model system of TiO_2/CdS QDSCs. When the electrolyte is replaced from polysulfide to $[Co(bpy)_3]^{2+/3+}$ complex, higher V_{oc} and η are observed because of its low redox potential. To resolve the slow diffusion nature of $[Co(bpy)_3]^{2+/3+}$ complexes within dense TiO_2 nanoparticle/CdS film, TiO_2 nanorod (NR) arrays anode is taken which increases η by more than a factor of 3. In addition, introduction of hexanoid acid (HA) in TiO_2 NR /CdS film is found to improve η (J_{sc} as well as V_{oc}) by alleviating the back recombination loss between Co^{III} and TiO_2 surface. Electrochemical impedance spectroscopy supports that the charge transfer resistance on the photoanode decreases by suppressing the interfacial charge recombination after HA treatment although adding HA in the electrolyte impedes diffusion resistance.

1. Introduction

Quantum dot solar cell (QDSC) has got attention as an alternative to silicon based solar cell because of easy tuning of band gap,[1] high extinction coefficient of quantum dot (QD),[2] possible application for transparent devices, and low cost. In QDSC, QDs harvest solar light and generate electron-hole pairs which are separated to an anode and an electrolyte. The anode is typically consisted of a wide band gap semiconductor such as TiO_2, and the electrolyte contains redox chemicals. Therefore, QDSCs are analogous to dye sensitized solar cells (DSSCs) in which a dye absorbs light instead, and inorganic QDs can have various advantages over organic dyes including durability under illumination. In addition, control of quantum confinement effect gives wide options to tailor their band gap, and QDs can be grown on the anode material.

However, low stability of QDs toward chemically corrosive iodine electrolyte (I^-/I_3^-), a popular electrolyte in DSSC, requires development of an electrochemical redox couple, suitable for QDSC. For example, a polysulfide redox couple (S^{2-}/S^0) based electrolyte has been mainly used for QDSC instead of an iodine electrolyte. Recently, a new generation of electrolytes including cobalt polypyridine complexes (bypyridine, terpyridine, phenathroline, and etc.), have been suggested as good electrolytes for QDSCs as well as DSSCs because of their non-corrosiveness[3] and their low redox potentials (0.43~0.85 V),[4,5] compared to the redox potential of polysulfide (0.55V).[2] The lower redox potential can give the higher open circuit potential (V_{oc}) of the solar cells.

However, only few studies have demonstrated the cobalt polypyridine electrolyte for QDSCs. For the success with the cobalt polypyridine electrolyte, two main problems, slow diffusivity of Co polypyridine complexes, and fast back recombination between Co^{III} species to electron in TiO_2, must be solved. It is reported that bulky Co complexes retard the diffusion toward the QD surface which limits the overall power conversion efficiency of the solar cells since photogenerated holes cannot transfer from QD to Co^{II} complex efficiently.[6] Therefore, the suitable pore size of TiO_2/QD film is required for fast charge transfer between QD and Co polypyridine complex. Porous or one-dimensional (1-D) TiO_2 nanostructures are promising for feasible diffusion of Co complex within the TiO_2/QD film, and single crystalline 1-D structures are favourable in terms of an electron transport across the anode. Secondly, negatively charged TiO_2 strongly interacts with positive Co^{III} ions, which causes strong back recombination and decreases the efficiency of the solar cells. To prevent the direct interaction and suppress the recombination between TiO_2 surface and Co complex, blocking close approach of Co complex toward TiO_2 surface would be helpful.[7] M. Ohta et al. reported that bulky alkylchain substitute in dye can reduce the back recombination.[8]

Alternatively, passivation of TiO_2 surface with long alkyl chain is expected to block the direct interaction with Co complexes. To demonstrate this idea, we introduced a straight alkyl chain molecule such as hexanoic acid (HA) to CdS sensitized TiO_2 film to keep a space between TiO_2 and Co^{III}, and studied its influence on the QDSC performances. For the model system,

$[Co(bpy)_3]^{2+/3+}$ (bpy = 2,4'-Bipyridine) based electrolyte was chosen since it is a simple and widely studied Co complex, and 1-D TiO_2 nanostructures were used for the anode.

In this study, polysulfide and $[Co(bpy)_3]^{2+/3+}$ complex electrolyte were compared for QDSCs, and the 1-D nanostructured TiO_2 anode was chosen for the $[Co(bpy)_3]^{2+/3+}$ electrolyte due to its diffusion issue. Finally, we demonstrate that the introduction of the long alkyl chain molecule, HA, in Co complex based CdS/TiO_2 QDSCs can improve the power conversion efficiency by alleviating the back recombination between Co^{III} and 1-D TiO_2, as a passivation layer.

2. Experimental section

To enhance the performance of QDSCs, the TiO_2 anodes were prepared and compared with nanoparticles (NP) and nanorods (NR) geometries. A TiO_2 NP film was prepared on an FTO substrate by the doctor blade technique using a 20 nm TiO_2 NP paste (TTP-20N, ENB Korea) and was annealed at 450 ºC for 1 hr to remove any organic binders inside the TiO_2 paste. A TiO_2 NR electrode was prepared by reported hydrothermal method.[8] A mixture solution of concentrate HCl (30 ml, Sigma-Aldrich, 37%), 3rd distilled water (30ml), and titanium isoprpoxide (2ml, Sigma-Aldrich, 97%) was stirred and transferred to a Teflon liner. A clean FTO substrate was dipped in the solution, and the reaction was performed with a stainless steel hydrothermal reactor at 200 ºC for 2 hr. TiO_2 NR grown on the FTO glass was washed and annealed at 400ºC in air for 1hr before CdS deposition. CdS QDs were deposited on TiO_2 NP and NR films, respectively, by a successive ionic layer adsorption and reaction (SILAR) method. TiO_2 film was dipped in 0.05M $Cd(NO_3)_2$ (Kanto chemical, 98%) and 0.05M Na_2S (Sigma-Aldrich) aqueous solution alternatively for 2 min, which were repeated by 14 cycles. TiO_2/CdS film were washed and dried by nitrogen gas blowing.[10] To introduce HA molecules on the electrode for some samples, the CdS sensitized TiO_2 NR film was soaked in 0.1M HA (Sigma-Aldrich, 99.5%) ethanol (J.T. baker, 99.9%) solution for 24hr.

To compare the performances of QDSCs by changing an electrolyte from a polysulfide electrolyte to a Co polypyridine electrolyte, we prepared two kinds of electrolytes. The polysulfide electrolyte was composed of 1M S (Kanto chemical, 99.5%) and 1M Na_2S (Sigma-Aldrich) solution in 7 : 3 volume ratio mixture of methanol (J.T. baker, 99.9%) and 3rd distilled water.[11] For the Co polypyridine electrolyte, a simple and widely used $[Co(bpy)_3]^{2+/3+}$ electrolyte was prepared. $[Co(bpy)_3](PF_6)_2$ was synthesized by following literatures.[11] 3.3 equimolar of 2,2'-bypiridyl (Sigma-Aldrich, 99%) was added to 1eq of $CoCl_2 \cdot 6H_2O$ (Sigma-Aldrich, 98%) methanolic solution, then excess amount of NH_4PF_6 (Sigma-Aldrich, 99.99%) was added, which were filtered and dried in vacuum oven for 24 hr. Then, 0.2M $[Co(bpy)_3](PF_6)_2$, 0.02M $NOBF_4$ (Sigma-Aldrich, 95%), 0.2M 4-tert-butyl pyridine (Sigma-Aldrich, 96%) and 0.2M $LiSO_3CF_3$ (Sigma-Aldrich, 99.995%) was prepared in acetonitrile (J.T. baker, 99.9%). Some of case, 0.01M HA (Sigma-Aldrich, 99.5%) was added as an additive in electrolyte.

QDSCs were assembled with a TiO_2/CdS film on the FTO substrate, a counter electrode of a Pt coated FTO glass (Solaronix), and a spacer (60 μm, Solaronix, Meltonix 1170-60) by hot pressing. The active area of the working electrodes was controlled to be 0.5 × 0.5 cm^2.

The morphologies of TiO_2/CdS NP and NR films were characterized by scanning electron microscopy (SEM) (Hitachi, S-4100), and crystal information of CdS sensitized TiO_2 film was confirm by X-ray diffraction method (XRD) (Shimaz, XRD-6000). Transmittance spectrum was obtained using a UV-Vis spectrometer (Varian, Cary 100).

Power conversion efficiency of QDSC was measured under 1 sun condition (100 mW/cm^2) which was simulated by a solar simulator (Abet Technologies, Sun 2000 Solar Simulator) equipped with an AM 1.5 filter. Further electrochemical analysis was performed through electrochemical impedance spectroscopy (EIS), carried out using a potentiostat (Ivium Technologies, IviumStat). EIS was measured at 500 kHz to 0.01 Hz under applied open circuit voltage with 1 sun illumination, and a fitting software (Zview, 2.8d version) was used.

3. Results and Discussion

The morphologies of TiO_2/CdS films were investigated by SEM (Fig. 1). The TiO_2 NR arrays were aligned on the FTO film, and their average length was 1.2 μm according to the cross sectional SEM images (Fig. 1A) which also shows that spaces are allowed between in the NR arrays. Meanwhile, TiO_2 NP film with sensitized CdS QD was densely packed (Fig. 1C and D).

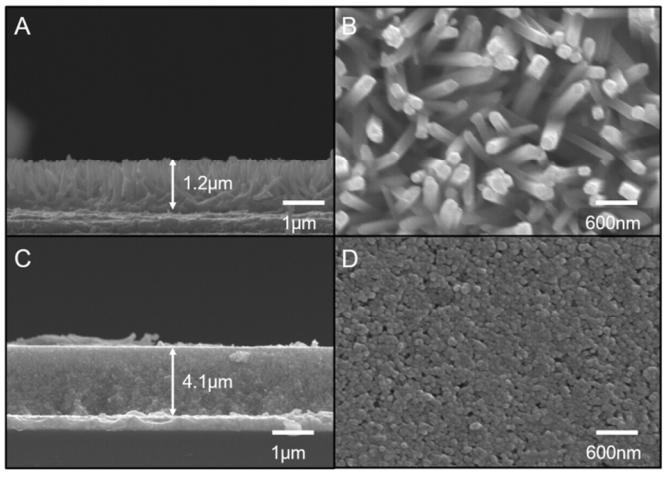

Figure 1. (A,B) Cross-sectional and top-view SEM image of TiO_2 NR/CdS, and (C,D) TiO_2 NP/CdS.

XRD patterns of TiO_2/CdS films confirmed the TiO_2 crystal structures, but, unfortunately, no peaks associated to CdS were observed due to a small amount of CdS. TiO_2 NP film had an

anatase phase, same as the TiO_2 paste that we used. Meanwhile TiO_2 NR arrays had a rutile phase, consistent with the previous studies. The present hydrothermal method gave only rutile phase on the FTO glass, due to the small lattice mismatch between FTO and rutile TiO_2.[8]

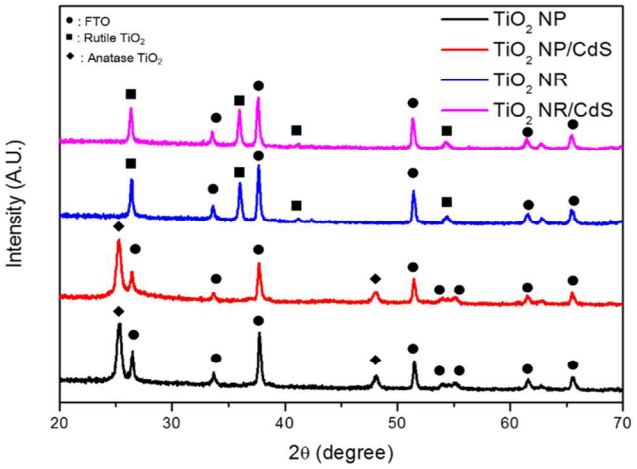

Figure 2. XRD patterns of TiO_2 NP, TiO_2 NP/CdS, TiO_2 NR, and TiO_2 NR/CdS showing anatase and rutile structure for NP and NR, respectively.

Additionally, these disparities in terms of the film density and TiO_2 crystal structures are believed to influence on the amount of the final sensitized CdS QD on TiO_2 surface according to UV-vis spectra (Fig. 3) and SEM EDS data (Fig. S1). The transmittance of TiO_2 NP/CdS showed that CdS QD fully absorbed the light, shorter than λ=500 nm. In contrast, partial absorption of the light (large transmittance) was observed with TiO_2 NR/CdS film although the same number of SILAR cycles was applied. Fig. S1, EDS results also showed the relatively lower atomic ratio of Cd/Ti on rutile TiO_2 NR than anatase NP. This means the smaller amount of CdS QD on NR film if it is considered that TiO_2 NP film was denser and thicker, thus had more amounts of materials according to the SEM images (Fig. 1). Although the amounts of CdS QDs was smaller on the NR film, Fig 3(B) showed that higher power conversion efficiency with TiO_2 NR/CdS QDSCs having both of higher J_{sc} and V_{oc}. When $[Co(bpy)_3]^{2+/3+}$ electrolyte is used, we expect that spaces in NR arrays allow easy diffusion of Co complex molecules and facile electron transport to CdS QD. Therefore, we expect that 1-D structure is favourable to the dense NP film for the Co based electrolyte. In addition, we confirmed that the power conversion efficiency of TiO_2 NR/CdS QDSCs was higher when the $[Co(bpy)_3]^{2+/3+}$ electrolyte was used instead of polysulfide electrolyte, due to the lower redox level of $[Co(bpy)_3]^{2+/3+}$ compared to S^{2-}/S^0. This difference in a redox potential level resulted in the higher V_{oc} and fill factor with the $[Co(bpy)_3]^{2+/3+}$ electrolyte. (Table 1)

Now, we tried to enhance the J_{sc} values to achieve higher power conversion efficiency with the $[Co(bpy)_3]^{2+/3+}$ electrolyte based QDSCs. J_{sc} can be improved by suppressing the recombination loss even with the same absorption efficiency. Therefore, to prevent the back recombination at the interface between TiO_2 and cobalt electrolyte, we added HA molecules on the photoanode or the cobalt electrolyte. T. Daeneke *et al.* reported that chenodeoxycholic acid as an additive increased J_{sc} and V_{oc} with a ferrocene electrolyte. They suggested chenodeoxycholic acid established a steady-state equilibrium between surface-adsorbed and electrolyte-borne, that surface adsorbed molecule block interfacial charge recombination.[12] P. Salvatori. *et al.* also observed similar behaviour of chenodeoxyholic acid in the $[Co(bpy)_3]^{2+/3+}$ electrolyte from experimental and computational results.[13]

The I-V performances of QDSCs depending on the HA usage are shown in Fig. 4. Unexpectedly, Cell d containing HA additive in the electrolyte, showed that both of V_{oc} and fill factor decreased slightly compared to Cell b. It is considered that high viscosity of HA exacerbates slow diffusion of cobalt complex molecules and decreases the cell performance. However, when HA was treated on the photoanode surface (Cell e), enhancement in J_{sc} was noticeable not only V_{oc}. It is possible if surface adsorbed HA molecules block the charge recombination similarly to chenodeoxycholic acid. If HA adsorption/desorption establishes steady-state equilibrium

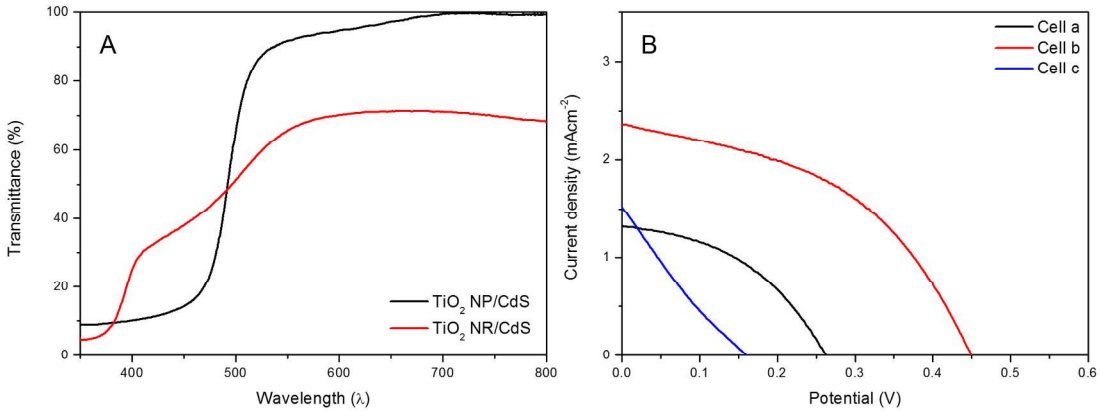

Figure 3. (A) UV-Vis spectrum of CdS sensitized TiO2 NR and NP; (B) I-V curve of QDSC. Cell a, TiO_2 NP/CdS photoanode with $[Co(bpy)_3]^{2+/3+}$; Cell b, TiO_2 NR/CdS photoanode with $[Co(bpy)_3]^{2+/3+}$; Cell c, TiO_2 NR/CdS photoanode with $S^{2-/0}$.

Table 1. Parameter of QDSCs with the conditions for the photoanode and the electrolyte

Cell	Photoanode	Electrolyte	J_{sc} (mAcm^{-2})	V_{oc} (V)	ff (%)	η (%)
a	TiO_2 NP/CdS	$Co(bpy)_3^{2+/3+}$	1.334	0.2634	41.98	0.1474
b	TiO_2 NR/CdS	$Co(bpy)_3^{2+/3+}$	2.312	0.4502	45.84	0.4771
c	TiO_2 NR/CdS	$S^{2-/0}$	1.519	0.156	20.13	0.0383
d	TiO_2 NR/CdS	$Co(bpy)_3^{2+/3+}$ with HA	2.389	0.4303	36.52	0.3753
e	TiO_2 NR/CdS/HA	$Co(bpy)_3^{2+/3+}$	2.795	0.4581	45.27	0.5796
f	TiO_2 NR/CdS/HA	$Co(bpy)_3^{2+/3+}$ with HA	2.480	0.4284	37.10	0.3942

between surface and electrolyte, adding extra HA in the electrolyte may shift equilibrium state toward more adsorption resulting in improved cell performances. We tested to use surface-adsorbed photoanode with combination of HA in the electrolyte together (Cell f). However, addition of HA harms the power conversion efficiency same as Cell d, detail I-V parameters of QDSCs are listed in table 1. It may imply that, extra HA only hindered diffusion of cobalt redox couples, rather than affected adsorption equilibrium of HA molecules on TiO_2 surface.

Interestingly, in a set of control experiments with NP TiO_2 QDSCs, adding HA both in the electrolyte and on the electrode showed an improved performance (Fig. S2). The different behaviour is considered to be originated from several reasons. Firstly, NP and NR had different TiO_2 crystal structures which can have different chemical properties. TiO_2 NP had an anatase structure while NR had a rutile structure. A stronger interaction of carboxylic acid functional group was reported with rutile TiO_2 than anatase.[14,15] In case of anatase, weak interaction between HA and TiO_2 surface can cause desorption of the molecules which requires extra HA in the electrolyte to interact back and forth. Meanwhile, extra HA is considered not to help for rutile TiO_2 NR due to its strong interaction, but rather to increase the viscosity of the electrolyte resulting in poorer diffusion of redox couples. Next, different morphology of NP and NR including the porosity and thickness of the film can result in the opposite trends for HA addition in the electrolyte. NP film was thicker and dense, which was expected to cause more back recombination since diffusion of cobalt complex ions across the film would be more interrupted compared to NR film. Then, recombination can be suppressed in NP film electrode more effectively than NR film with the usage of HA, and even HA molecules in the electrolyte might result in improved cell performance with NP film. Therefore, a careful strategy is required to be chosen by considering the TiO_2-molecule interaction.

The influence of HA on the cell performance was discussed more with an EIS measurement. The measured data (dot) and the fitted data (line) of each cell are shown (Fig. 5 and Table 2). The equivalent circuit implies components of the QDSC; sheet resistance (R_s), charge transfer on photoanode (R_1), charge transfer on cathode (R_2), and diffusion resistance (R_w).

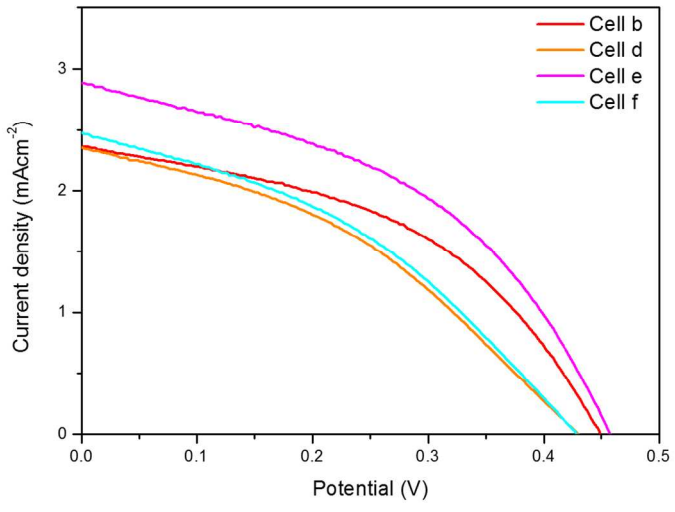

Figure 4. I-V curves of various QDSCs depending on the use of the HA; No HA was contained (Cell b), HA was added in the electrolyte (Cell d), the TiO_2/CdS electrode was soaked in HA before cell assembly (Cell e), and HA was applied for both on the TiO_2/CdS electrode and the electrolyte (Cell f).

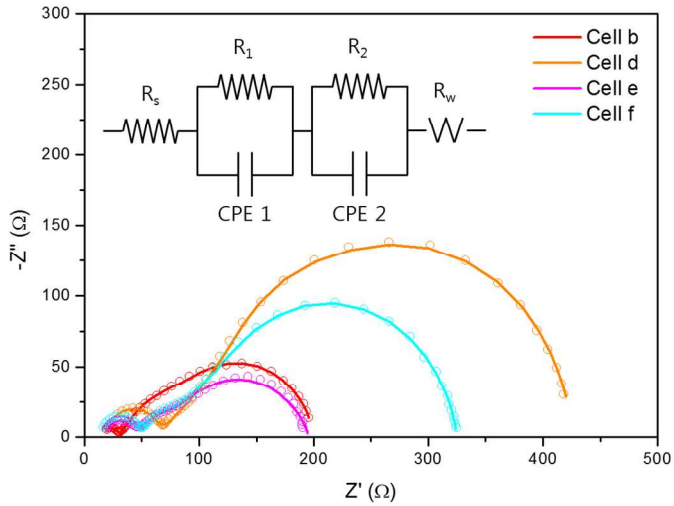

Figure 5. Electrochemical impedance spectroscopy of QDSCs. Inset figure is an equivalent circuit for the fitting.

Table 2. Fitted value from EIS spectra shown in Fig. 5

Cell	R_s	R_1	R_2	R_w	n_w
b	16.32	24.81	11.57	147.9	0.43
d	15.93	20.27	48.04	341.4	0.47
e	15.49	8.42	26.86	145.3	0.37
f	13.44	13.34	33.28	265	0.45

Comparing Cell b (without HA) and Cell e (surface absorbed HA), charge transfer resistance on the photoanode, R_1, meaningfully decreased from 24.81Ω to 8.42 Ω because HA blocks interfacial charge recombination as we expected. On the other hand, diffusion resistance of Cell d (additive HA to the electrolyte only), R_w, increased more than twice from that of Cell b which is consistent with our expectation based on the I-V performance results, that HA aggravates slow diffusion of cobalt redox couples probably due to high viscosity of HA. In case of Cell f (addition of HA both in the electrolyte and on the electrode), decreased R_2, but increased R_w was observed. EIS interpretation is well matched with I-V results and our suggestion, which the introduction of HA had trade-off effects on charge recombination and diffusion of $Co^{2+/3+}$.

Additionally, the stability of our best performing QDSC was tested compared with the Cell c, a typical QDSC using the polysulfide electrolytes. The normalized current by each initial J_{sc} was monitored over 1000 sec without external potential. Photocurrents both of Cell c and Cell e decreased slightly under the simulated sunlight illumination. In case of QDSCs, photo-bleaching of CdS was attributed to decrease of the photocurrents, and we observed similar level of decrease with Cell c and Cell e, regardless of the type of the electrolyte between polysulfide and cobalt based electrolytes. It can imply that the condition of Cell e is as stable as polysulfide electrolyte. A sharp peak of photocurrent was observed with Cell e under chopped illumination condition, induced by slow diffusivity of large cobalt polypyridine molecules.[5]

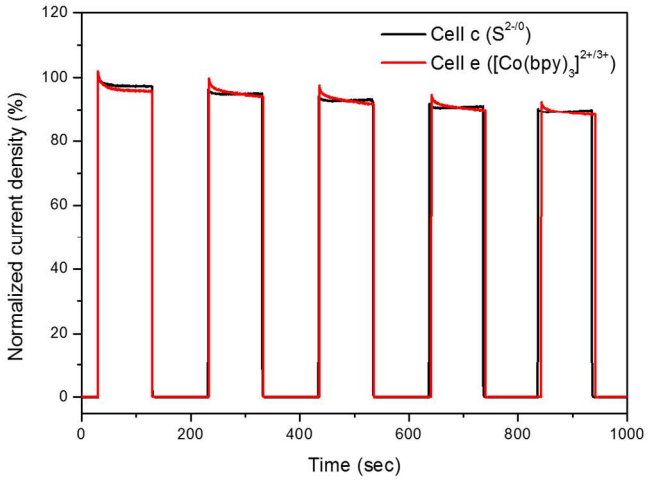

Figure 6. Photocurrents without external potential by time showing similar levels of stability. Cell c, and Cell e were composed of the polysulfide, and the cobalt based electrolyte, respectively.

Conclusions

We demonstrate that the power conversion efficiency of TiO_2/CdS QDSCs can be enhanced by varying electrolytes, and nanostructures of TiO_2 anode, and using an additive molecule. Low redox potential of cobalt bipyridine based electrolyte contributed to increase V_{oc}, and with this electrolyte, 1-D TiO_2 NR/CdS QD arrays performed better than NP structures by noticeably increasing both of J_{sc} and V_{oc}. With higher power conversion efficiency, the cobalt bipyridine electrolyte based QDSC was as stable as polysulfide electrolyte based one. In addition, further enhancement of J_{sc} as well as V_{oc} was achieved by treating HA on the TiO_2 NR/CdS surface, and EIS data suggested that the interfacial charge recombination between the Co electrolyte and TiO_2 was suppressed when HA was added as a blocking layer. The interaction between TiO_2 to HA determined the influence of addition of HA in the electrolyte or adsorption on the surface. Here, we demonstrate the positive contribution of HA, a molecule having a long alky chain, in the QDSC performance, when the back recombination at the junction between the electrolyte and the anode was problematic.

Acknowledgements

This research is funded by the institutional program of Korea Institute of Science and Technology (KIST)

Notes and references

[a] *Clean Energy Research Center, Korea Institute of Science and Technology (KIST), 39-1 Hawolgock Dong, Seoul 136-791, Republic of Korea, Fax:82-2-958-5219*

[b] *Department of Chemistry, Korea University, Seoul 136-713, Republic of Korea*

[c] Department of Clean Energy and Chemical Engineering, Korea University of Science and Technology, Daejeon 305-350, Republic of Korea

*Corresponding author Email addresses: *joocat@kist.re.kr*
**Corresponding author Email addresses: *yjhwang@kist.re.kr*

† Electronic Supplementary Information (ESI) available: [SEM-EDS data and the cell performance of TiO_2 nanoparticle based QDSCs depending on HA usage are included]. See DOI: 10.1039/b000000x/

1. P. V. Kamat, *J. Phys. Chem. C*, 2008, **112**, 18737-18753.
2. J. B. Sambur, T. Novet and B. A. Parkinson, *Science*, 2010, **330**, 63-66.
3. K. Miettunen, T. Saukkonen, X. E. Li, C. Law, Y. K. Sheng, J. Halme, A. Tiihonen, P. R. F. Barnes, T. Ghaddar, I. Asghar, P. Lund and B. C. O'Regan, *J. Electrochem. Soc.*, 2013, **160**, H132-H137.
4. J.-H. Yum, E. Baranoff, F. Kessler, T. Moehl, S. Ahmad, T. Bessho, A. Marchioro, E. Ghadiri, J.-E. Moser, C. Yi, M. K. Nazeeruddin and M. Grätzel, *Nat. commun.*, 2012, **3**, 631.
5. S. M. Feldt, G. Wang, G. Boschloo and A. Hagfeldt, *J. Phys. Chem. C*, 2011, **115**, 21500-21507.
6. J. J. Nelson, T. J. Amick and C. M. Elliott, *J. Phys. Chem. C*, 2008, **112**, 18255-18263.

7. E. Mosconi, J. H. Yum, F. Kessler, C. J. G. Garcia, C. Zuccaccia, A. Cinti, M. K. Nazeeruddin, M. Gratzel and F. De Angelis, *J. Am. Chem. Soc*, 2012, **134**, 19438-19453.
8. M. Ohta, N. Koumura, K. Hara and S. Mori, *Electrochem. Commun.*, 2011, **13**, 778-780.
9. Y. J. Hwang, C. Hahn, B. Liu and P. D. Yang, *Acs Nano*, 2012, **6**, 5060-5069.
10. S. S. Kalanur, S. Y. Chae and O. S. Joo, *Electrochim. Acta*, 2013, **103**, 91-95.
11. S. Y. Chae, Y. J. Hwang, J.-H. Choi and O.-S. Joo, *Electrochim. Acta*, 2013, **114**, 745-749.
12. T. Daeneke, T. H. Kwon, A. B. Holmes, N. W. Duffy, U. Bach and L. Spiccia, *Nat. Chem.*, 2011, **3**, 211-215.
13. P. Salvatori, G. Marotta, A. Cinti, C. Anselmi, E. Mosconi and F. De Angelis, *J. Phys. Chem. C*, 2013, **117**, 3874-3887.
14. A. Mattsson and L. Osterlund, *J. Phys. Chem. C*, 2010, **114**, 14121-14132.
15. R. Luschtinetz, S. Gemming and G. Seifert, *Eur. Phys. J. Plus*, 2011, **126**.

